ION SOURCE DEVELOPMENT

IN THE CULHAM LABORATORY OF AEA TECHNOLOGY

A J T Holmes
AEA Technology, Culham, Abingdon, Oxfordshire, OX14 3DB, UK

1. INTRODUCTION

Over the past eighteen years, Culham has been developing ion sources for various applications. In general these sources have had the task of injecting the maximum current into a defined solid angle which in effect defines a beam brightness and, more specifically, defines a beam current and emittance. Initially these sources were for producing proton beams for fusion heating experiments and more recently for H^- beams.

In this paper I describe the present achievements for both types of source and show how the same technology can be adapted for intense beams of both kinds of ion. There is a very close relationship between the production of H^- and H^+ which can be exploited to produce a high brightness beam of either ion. The paper also describes the accelerator technology and emittance of these beams. The ion source technology has been developed for continuous operation but it is possible to modulate the ion beam at frequencies up to 1 kHz using the source and in excess of 1 MHz using beam deflectors. A description of a novel low energy transport channel to the RFQ or DTL are also given.

2. THE PLASMA SOURCE

In this paper I will focus solely on the magnetic multipole or bucket ion source. This is shown in figure 1 and is a simple box lined on all sides except the extraction plane by rows of permanent magnets arranged in a N-S-N pattern as seen in figure 1. This box is the anode of the discharge and there are a number of hot wire filaments which act as cathodes. These filaments are usually heated by ac currents and are arranged in groups of three to minimise ripple. They are located at the back of the source, away from the extraction plane. The discharge forms between the anode and cathodes and is confined from the anode by the high order multipole magnetic fields. As a result a dense plasma forms ($n \geq 10^{12}$ cm^3) for arc currents in excess of 100 A/litre of volume. The discharge voltage is typically 100 V in H_2 pressures of a few millitorr.

However discharges in simple sources such as I have just described usually produce only low densities of H^+ or H^- ions. This arises from the fact that H^+ or H^- forms only in two-step ionisation processes. For H^+ formation the normal channel is:

$$\begin{aligned} e(E>15eV) + H_2 &\rightarrow H_2^+ + 2e \\ e(E<5eV) + H_2^+ &\rightarrow H^+ + H + e \\ H_2^+ + H_2 &\rightarrow H_3^+ + H \\ e(E<5eV) + H_3^+ &\rightarrow H^+ + 2H + e \end{aligned}$$

A small amount of protons are formed directly by:

$$e(E>13eV) + H \rightarrow H^+ + 2e$$

To form a high fraction H^+ we must stop the ionisation process by excluding fast electrons and allow molecular ion break up by slow electrons.

A similar requirement exists for H^- production via dissociative attachment to vibrationally excited molecules, $H_2(v)$. Hence

$$\begin{aligned} e(E>13eV) + H_2(v=o) &\rightarrow H_2(v>6) + e \\ e(E\sim1eV) + H_2(v>6) &\rightarrow H^- + H \\ e(E>3eV) + H^- &\rightarrow H + 2e \end{aligned}$$

Again the presence of fast and slow electrons is essential with the fast electrons again being excluded from H^- production region to minimise H^- losses. This can be achieved by the magnetic filter.

2.1 The Magnetic Filter

This is shown again in figures 1 and 2. It is essentially a sheet of magnetic field separating two relatively field-free regions of plasma. Figure 1 shows an azimuthally symmetric system while figure 2 shows the simpler dipole type of filter. It works by modifying the diffusion coefficient of electrons in the plasma which is given by:

$$D_e = \frac{\nu kT}{m(\nu^2 + \omega^2)}$$

where kT = electron thermal energy
ν = collision frequency = $C\,T^{-3/2}$
ω = cyclotron frequency = eB/m
m = electron mass

Away from the filter we have $\omega = 0$, so:

$$D = \frac{kT^{5/2}}{mC}$$

while in the filter region $\omega >> \nu$, so:

$$D = mCkT^{-1/2}/e^2B^2$$

This means the normal order of events is reversed in the filter, fast electrons diffuse more slowly than slow electrons so we have a Maxwell's demon. Thus, dependent on the strength of B, we can choose the electron energy beyond the filter.

The requirements for proton production are not so stringent as for H^- production. In the former case we have to merely stop ionisation and have sufficient depth of plasma (typically 5 cm) such that molecular ions (for example H_2^+ and H_3^+) are broken up. In the latter case

we must exclude virtually all electrons whose energy exceeds 2 eV. Thus the filter for H11- production must have a higher value of $\int B^2 dl$, typically 5000 gauss^2 cm.

2.2 Proton Sources

Two fully developed proton sources have been designed and tested; the JET PINI source (55 x 31 x 22 cm^3) and the demonstrator source (18 x 30ϕ cm^3) which is also an H^- source. I will focus on the latter as it has a higher proton yield and is more suitable for single aperture applications. The proton yield is shown in figure 3 as a function of discharge current. At an ion current density of 100mA/cm^2, the proton yield is 87% (that for the PINI is only 80%). Higher proton fractions are possible with even stronger filters at the price of a lower available current density (because of the reduced value of the diffusion coefficient).

The discharge in long pulse mode is limited to around 80 A per filament (240 A) although this source has not been tested beyond about 140 A. The positive ion current density is linear with arc current over the full range. Higher discharge currents are feasible by adding extra filaments but accelerator perveance limitations limit j_+ to below about 200 mA/cm^2.

2.3 H^- Sources

In this case I will use the Type 4 H^- source as an example (19 x 10 x 10 cm^3 with three filaments). The extracted H^- current as a function of arc current is shown in figure 4. Unlike the proton source the H^- current tends to a limiting value and the peak value obtained for a 10 second pulse is 44 mA (22mA/cm^2) at an energy of 83 keV. Thus limitation is thought to be a result of the two step production process described earlier.

Addition of cesium as a catalyst adds an additional channel to the production process. We think this may be

$$Cs^* + H_2(v) \rightarrow Cs^+ + H^- + H$$

which overcomes the saturation effect. The effect on the discharge is shown in figure 5 where is can be seen that the H^- current is linear with arc current up to a maximum of 86 mA (43 mA/cm^2).

An additional problem with H^- sources is the suppression of co-extracted electrons. This is achieved by placing a transverse magnetic field across the aperture which effectively reduces the diffusion coefficient to a level where the electron flux is of the same order as the H^- current.

3. EMITTANCE

The beam emittance depends on many causes. These are:

- finite ion temperature in the plasma
- plasma ion emitting boundary aberrations
- accelerator aberrations
- LEBT emittance growth
- magnetic stochastic effects (H^- only)

We find no evidence for LEBT emittance growth or instabilities with multipole sources and the accelerator ray tracing codes show little sign of aberrations on transiting the accelerator. However the other three effects are non-trivial.

In earlier papers[1,2] I have shown that for a beam energy U and positive current density j_+ we have:

$$\varepsilon_n^2 = R^2 \left(\frac{1}{4} \left(\frac{T}{U} \right) + \frac{\gamma B^2 \lambda^2}{4U} + \alpha R^2 j^{2/3} / D^{2/3} \right)$$

where λ is the scattering length and R/D is the radius to extraction gap ratio. The first component arises from the finite ion temperature, T, the second component arises from the magnetic fields in the plasma and the last component depends on the plasma non-uniformity (also usually caused by the presence of magnetic fields. The second term is not usually very dominant unless these fields are very strong.

The above equation has been tested experimentally as seen in figure 6, where straight lines are obtained when ε_n^2 is plotted as a function of $j_-^{2/3}$ or $j_+^{2/3}$. This shows that the emittance of 8 mm radius H^- beams is 0.08 πmm mrad and rises with $j^{2/3}$ to a maximum of 0.26 πmm mrad. For He^+ beams (no proton data is available) the beam is largely dominated by its plasma temperature and the emittance is 0.02 πmm mrad.

4. THE ACCELERATOR

The accelerator is formed by a series of flat electrodes with circular apertures biased to potentials such that the beam gains the required energy and is collimated when it exits the last accelerating electrode. The first of these electrodes also forms one side of the plasma source as seen in figures 1 and 2. The beam is emitted from a curved plasma meniscus as seen in figure 7 which gives inward beam focusing. Subsequent electrodes create additional lenses of circular symmetry whose focal length is given by:

$$f^{-1} = (E_2 - E_1)/4U$$

where E_2 and E_1 are the downstream and upstream electric fields on either side of the electrode and U is the local beam energy.

It is possible to analyse the accelerator using matrix operators based on the above expression but it is much more convenient to analyse the problem using ray tracing codes such as IONTRAK which is a descendent of AXCEL. An example of the output is shown in figure 7 (note the geometry is distorted by conformal mapping).

The code can be used to analyse positive ion beams and also works very well for negative ion beams if the electron component is ignored. It models the ions from the plasma to the target and so forms the plasma meniscus self-consistently. This meniscus is responsible for a significant fraction of the total emittance growth if the plasma is non-uniform giving an aspherical shape to the meniscus.

5. THE LEBT

The beam transport to the RFQ requires two adjustable parameters per plane to match the beam emittance into the RFQ acceptance with maximum overlap. It is preferable to do this by circularly symmetric lenses as the accelerator gives at least one such lens as part of the acceleration process. Usually this is a solenoid just upstream of the RFQ. In addition beam alignment elements are also needed.

It is possible to use the accelerator alone to provide beam matching and alignment and a possible design is shown in figure 8. Here several extra lenses are created by having additional electrodes to create an accel-decel type structure. The focusing lenses become very strong under this situation and this particular example is designed for a 6° convergence into the RFQ, but is not fully optimised. Beam alignment is handled by segmenting one of the electrodes into four and applying weak dipole electric fields across the aperture to steer the main beam. Not shown in figure 8 is the electron separator which is two dipole magnets back-to-back which remove the H^- beam to be displaced sideways.

An advantage of this LEBT approach is compactness and simplicity and also the whole beamline path can be modelled by a single code IONTRAK, which eliminates many uncertainties.

6. CONCLUSIONS

Ion source development has now reached a stage that the requirements of future spallation sources can be met for both beam current and emittance for the initial beam. The novel designs of multipole sources lead to compact ion source systems whose power and cooling requirements are modest and can be operated over a wide range of beam pulse lengths, even continuous operation.

REFERENCES

1. Holmes A J T, Proc. IEEE Conf. on Particle Accelerators, Washington, p257, (1987).

2. Holmes A J T and Surrey E, Rev. Sci. Instrum., 62, p1173, (1991)

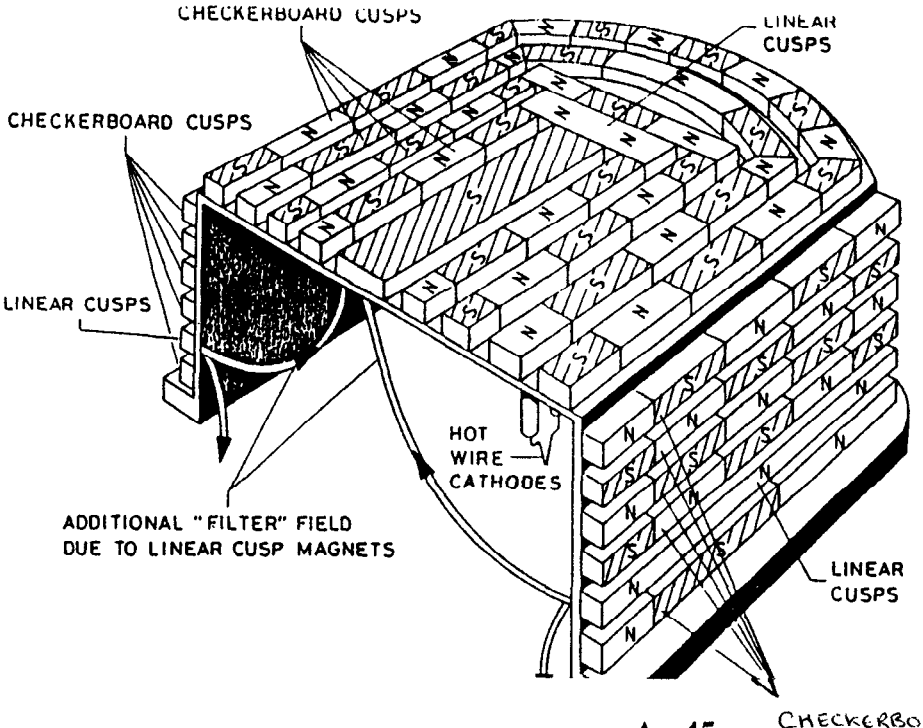

FIGURE 1

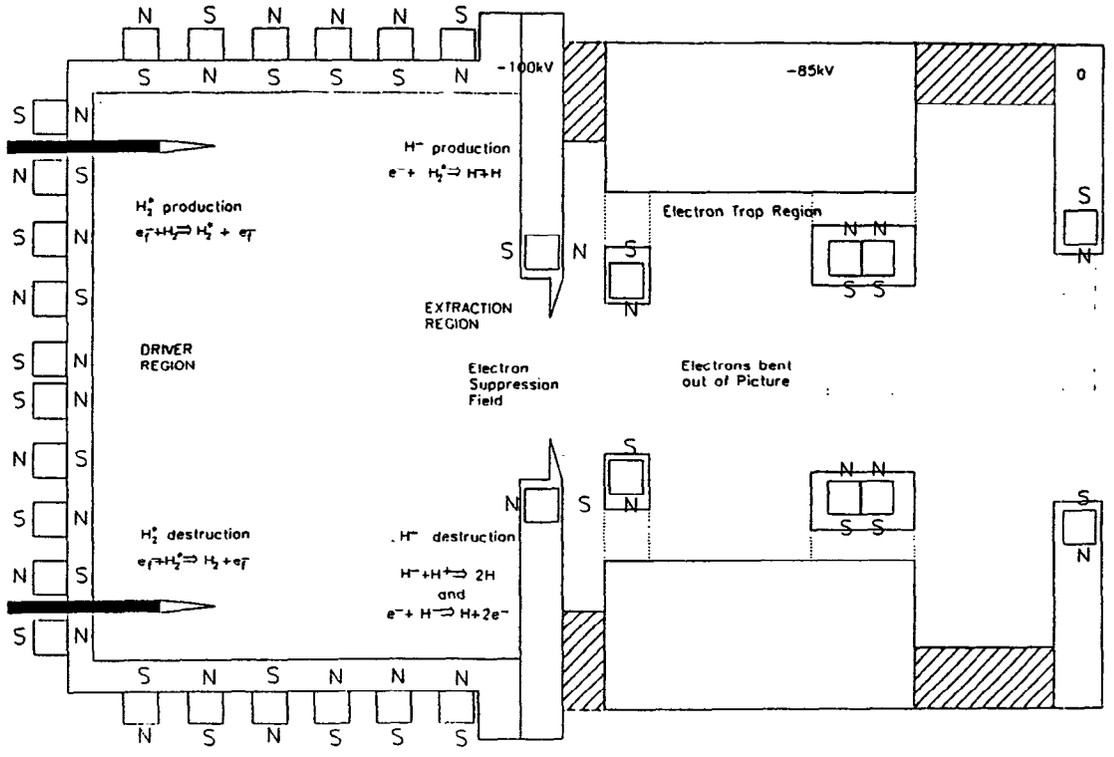

FIGURE 2

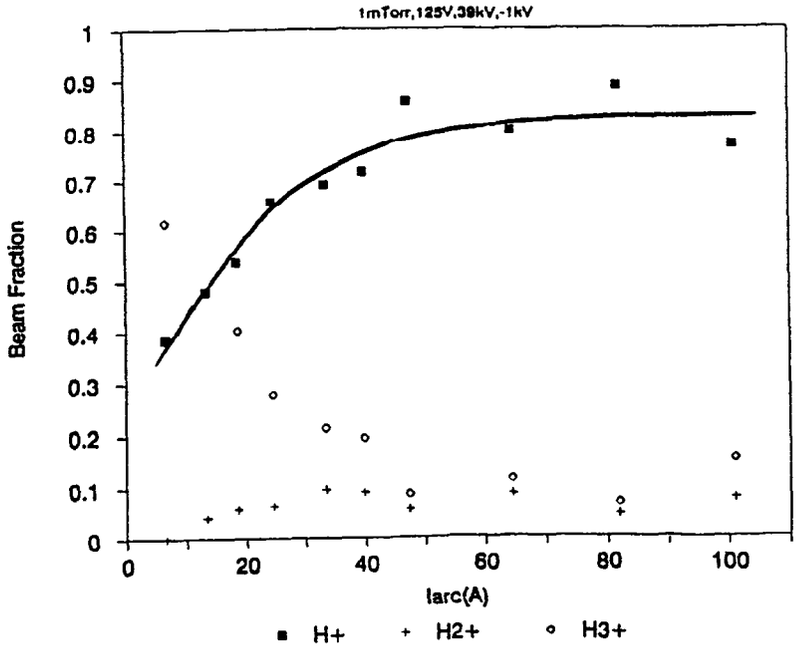

FIGURE 3

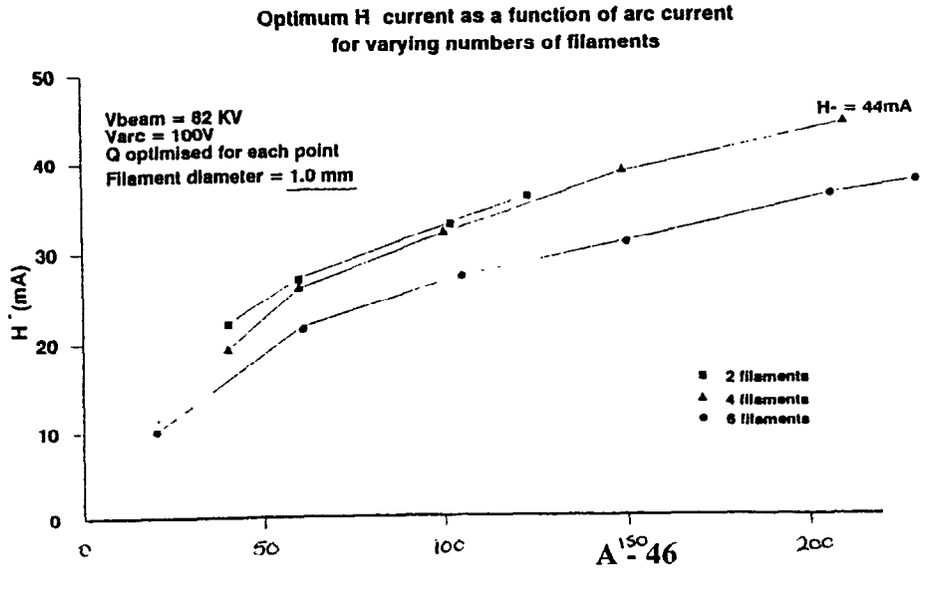

FIGURE 4

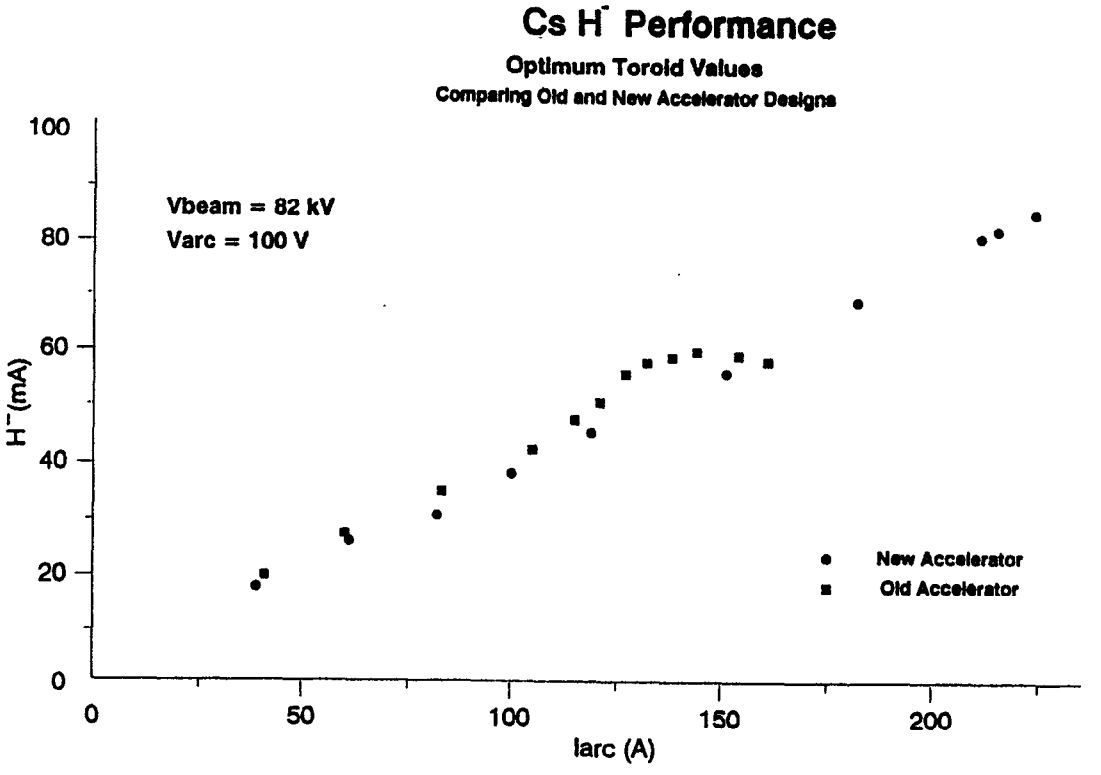

FIGURE 5

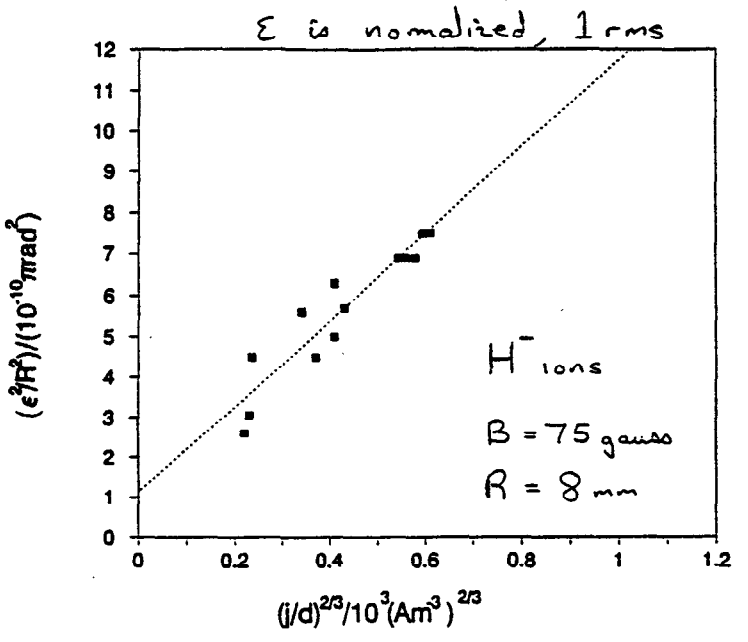

FIGURE 6

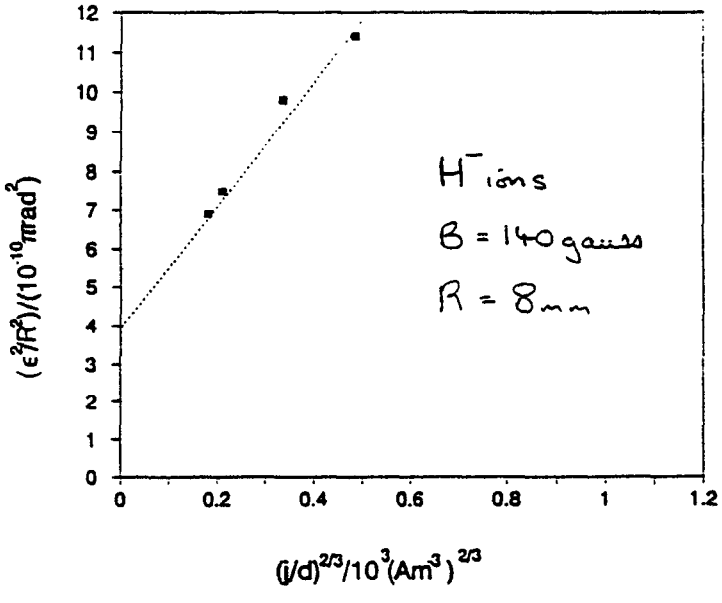

Current density = 100 mA/cm^2
Vext = 16KV
Vbeam = 90KV
Transported current = 220 mA

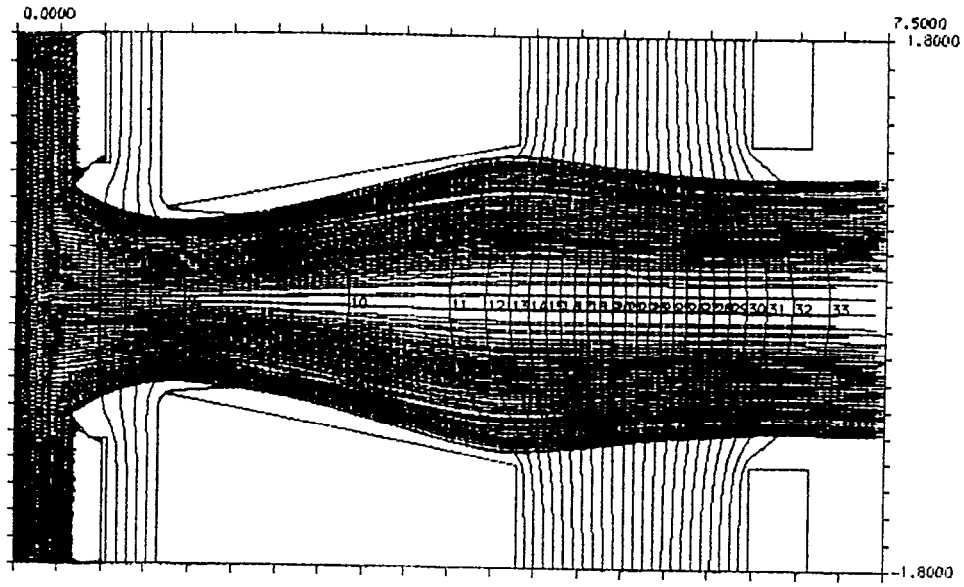

FIGURE 7

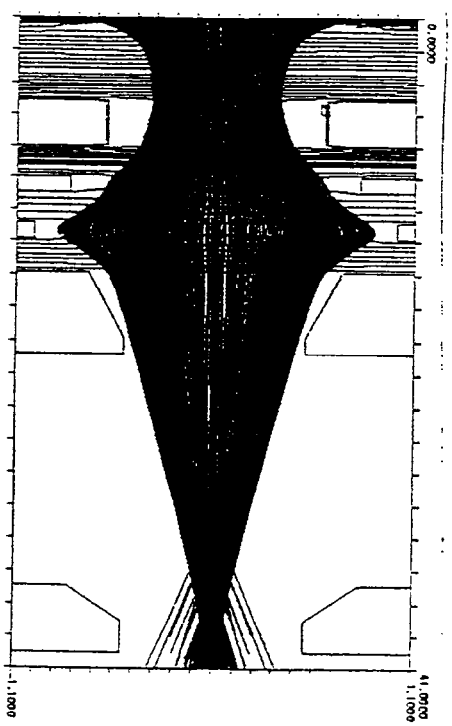

FIGURE 8